Acta Pharmacologica Sinica (2017) 38: 233–240
 1671-4083/17
www.nature.com/aps

Original Article

Efficacy of afatinib, an irreversible ErbB family blocker, in the treatment of intracerebral metastases of non-small cell lung cancer in mice

Shi-rong ZHANG[1, 2, #], Lu-cheng ZHU[1, 3, #], Yan-ping JIANG[1], Jing ZHANG[1], Ru-jun XU[4], Ya-si XU[1, 2], Bing XIA[3, *], Sheng-lin MA[1, 2, 5, *]

[1]Hangzhou Translational Medicine Research Center, Hangzhou First People's Hospital, Nanjing Medical University, Hangzhou 310006, China; [2]Hangzhou Translational Medicine Research Center, Affiliated Hangzhou First People's Hospital of Zhejiang Chinese Medical University, Hangzhou 310006, China; [3]Department of Oncology, Hangzhou Cancer Hospital, Hangzhou 310006, China; [4]Department of Pathology, Hangzhou First People's Hospital, Nanjing Medical University, Hangzhou 310006, China; [5]Department of Oncology, Hangzhou First People's Hospital, Nanjing Medical University, Hangzhou 310006, China

Abstract

Few effective therapeutic options are currently available for the treatment of non-small cell lung cancer (NSCLC) with brain metastases (BM). Recent evidence shows that NSCLC patients with BMs respond well to afatinib, but little is known about the underlying mechanisms. In this study, we evaluated the efficacy of afatinib in treatment of BMs in mice and investigated whether afatinib could actively penetrate the brain-blood barrier and bind to its target. NSCLC BM model was established in nude mice by intracerebral injection of PC-9.luc cells. The tumors were measured weekly using *in vivo* quantitative bioluminescence. The mice are administrated afatinib (15, 30 mg·kg^{-1}·d^{-1}, ig) for 14 d. The antitumor efficacy of afatinib was determined by tumor growth inhibition (TGI), which was calculated as [1–(change of tumor volume in treatment group/control group)×100]. Pharmacokinetic characteristics were measure in mice receiving a single dose of afatinib (30 mg/kg, ig). Pharmacodynamics of afatinib was also assessed by detecting the expression of pEGFR (Tyr1068) in brain tumor foci using immunohistochemistry. Administration of afatinib (15, 30 mg·kg^{-1}·d^{-1}) dose-dependently inhibited PC-9 tumor growth in the brain with a TGI of 90.2% and 105%, respectively, on d 14. After administration of afatinib (30 mg/kg), the plasma concentration of afatinib was 91.4±31.2 nmol/L at 0.5 h, reached a peak (417.1±119.9 nmol/L) at 1 h, and was still detected after 24 h. The cerebrospinal fluid (CSF) concentrations followed a similar pattern. The $T_{1/2}$ values of afatinib in plasma and CSF were 5.0 and 3.7 h, respectively. The $AUC_{(0-24\ h)}$ values for plasma and CSF were 2375.5 and 29.1 nmol/h, respectively. The plasma and CSF concentrations were correlated (r=0.844, P<0.01). Pharmacodynamics study showed that the expression levels of pEGFR were reduced by 90% 1 h after afatinib administration. The E_{max} was 86.5%, and the EC_{50} was 0.26 nmol/L. A positive correlation between CSF concentrations and pEGFR modulation was revealed. Afatinib penetrates the BBB in NSCLC BM mice and contributes to the brain tumor response. The CSF exposure level is correlated with the plasma level, which in turn is correlated with the modulation of pEGFR in the tumor tissues. The results support for the potential application of afatinib in NSCLC patients with BMs.

Keywords: afatinib; tyrosine kinase inhibitor; non-small cell lung cancer; brain metastasis; pharmacokinetic/pharmacodynamics; pEGFR

Acta Pharmacologica Sinica (2017) 38: 233–240; doi: 10.1038/aps.2016.107; published online 14 Nov 2016

Introduction

Approximately 200 000 brain tumor cases have been estimated to occur in the United States each year, most of which (160 000) are brain metastases (BMs)[1]. The prognosis of these patients after diagnosis is extremely poor. In cases of non-small cell lung cancer (NSCLC), 20%–40% of patients have BMs during the course of the disease[2]. Currently, whole-brain radiotherapy (WBRT) is the only approved standard of care for the treatment of BMs with central nervous system (CNS) symptoms[3]. No molecular targeted therapy has been approved for the treatment of NSCLC with BMs.

Afatinib is an orally available, irreversible ErbB family blocker approved in the European Union, the United States, and several Asian and Latin American countries for tyrosine

# These authors contributed equally to this work.
*To whom correspondence should be addressed.
E-mail mashenglin@medmail.com.cn (Sheng-lin MA);
xb0918@hotmail.com (Bing XIA)
Received 2016-04-18 Accepted 2016-08-23

kinase inhibitor (TKI)-naïve patients with epidermal growth factor receptor (EGFR)-mutated NSCLC. In contrast to the reversible EGFR-TKIs gefitinib and erlotinib, afatinib covalently binds to the ErbB receptor *in vitro*, thereby irreversibly blocking signaling and leading to sustained anti-mitogenic activity[4]. A recent analysis has reported that 35 patients with BMs from the LUX-Lung3 study who were treated with either first-line afatinib or cisplatin/pemetrexed showed a median progression-free survival (PFS) of 11.1 months with afatinib treatment compared with a PFS of 5.4 months with chemotherapy treatment (hazard ratio [HR], 0.54; P=0.138)[5]. Another study on the outcomes of pretreated NSCLC patients with CNS metastases who received afatinib within an Afatinib Compassionate Use Consortium (ACUC) has reported that thirty-five percent (11 of 31) of the evaluable patients had a cerebral response, sixteen percent (5 of 31) responded exclusively in the brain, and sixty-six percent (21 of 32) had cerebral disease control after treatment with afatinib[6]. Afatinib appears to penetrate the CNS at concentrations sufficiently high to exert a clinical effect on CNS metastases. Preclinically, a limited number of studies have demonstrated the relationship of afatinib exposure and efficacy in patients with BMs.

In the present study, we used a mouse model of BM, which was generated by using a stereotactic injection approach. We administered afatinib to normal mice and mice with BMs and evaluated the efficacy of afatinib in treatment of intracerebral NSCLC with activating EGFR-mutations, as well as the correlation of exposure to cerebrospinal fluid (CSF) and phosphorylated EGFR (pEGFR) modulations in tumors at different doses. We also attempted to address whether afatinib can actively penetrate the brain-blood barrier (BBB) and bind to its target.

Materials and methods

Cells and chemicals

PC-9 cells were obtained from the American Type Culture Collection (ATCC) and were routinely cultured in RPMI-1640 medium supplemented with 10% (v/v) fetal calf serum (Gibco, Carlsbad, CA, USA). All of the cells were maintained at 37 °C with 5% CO_2 under humidifying conditions. Afatinib (Cayman, San Diego, CA, USA) was dissolved in dimethyl sulfoxide (DMSO).

Drug administration

Afatinib was formulated in a 1% (v/v) solution of methylcellulose/Tween-80 in deionized water. For the tumor growth assay, 15 and 30 mg/kg afatinib, or vehicle control was given to mice once daily by oral gavage for 14 continuous days. For the pharmacokinetic (PK) and pharmacodynamics (PD) study, a single dose of vehicle control or 30 mg/kg afatinib was given to mice by oral gavage.

Viral transduction

PC-9 cells were transfected with HIV1-based lentiviral vector plasmid pHRSIN-CSGW-DINotI, which expresses firefly luciferase (luc) under the control of the spleen focus-forming virus promoter. Lentiviral vectors were generated by the transfection of 293T cells with plasmids encoding the vesicular stomatitis virus G envelope, gag-pol, and luc. Conditioned medium containing viral vectors was harvested 48 h post-transfection. PC-9 cells were transfected using viral supernatants. The stable clone was selected by limiting dilution and was cultured with the addition of 1 μg/mL puromycin. The expression of luc was confirmed via the measurement of luciferase activity using a Bright-Glo Luciferase Assay System (Promega). Detailed procedures are described in previous publications[7, 8]. The transfected cell line is referred to as PC-9.luc. The average level of luciferase activity per 5×10^4 cells was approximately 1500 relative light units.

Intracerebral BM non-small cell lung cancer model

Pathogen-free female athymic (nu/nu) mice, 6 to 8 weeks old, were obtained from Charles River (Beijing, China). All animal studies were approved by the Institutional Animal Care and Use Committee of Zhejiang Academy of Medical Sciences (Hangzhou, China), and the experiments were conducted according to the guidelines set by the National Research Council. The mice were acclimatized for 1 to 2 weeks before starting experiments. For tumor cell implantation, the mice were anesthetized with a ketamine/xylazine mixture. A 1-cm incision was made over the parieto-occipital bone, and the bregma was identified. A sterile 25-gauge sharp needle was used to puncture the skull 2 mm right lateral of the bregma and 1 mm anterior to the coronal suture. A total of 1.0×10^6 PC-9.luc cells were injected at a density of 1×10^5 cells/μL. After tumor cell inoculation, all of the mice were monitored using an IVIS Lumina imaging station (Caliper Life Sciences). Tumors were allowed to grow (the radiance intensity reached approximately 4×10^6 photons per second per steradian per square cm [photons/s/sr/cm^2]) before the administration of afatinib or vehicle control. In addition, to determine whether the tumor was successfully established in the brain, brain tissue was harvested 14 d after tumor cell injection, sliced into pathological sections and stained with hematoxylin and eosin (H&E). The integrity of the BBB was also determined after the injection of the tumor cells via an intracerebral injection of the nude mice. BM mice and normal mice (n=3 per time point for each group) were administered 30 mg/kg afatinib by oral gavage. At time points 0.5, 1, 2, 8, and 24 h after dosing, the animals were humanely sacrificed, and samples were harvested. CSF was collected by inserting a 1-mL syringe into the dura through the atlanto-occipital membrane at a 30° angle and was stored at -80 °C until PK analysis.

Tumor growth assay

The mice were randomized into three groups, which each received either vehicle control (n=5), 15 mg/kg afatinib (n=5), or 30 mg/kg afatinib (n=5). The tumors were measured weekly by *in vivo* quantitative bioluminescence. Imaging was conducted using an IVIS Lumina imaging station (Caliper Life Sciences). In preparation for imaging, the mice were simultaneously anesthetized with ketamine/xylazine and were administered luciferin (D-Luciferin potassium salt, 150

mg/kg, Caliper Life Sciences) via intraperitoneal injection; the mice were then imaged 10 min after the injection. The regions of interest (ROI) that encompass the intracranial area of the signal were defined using Living Image software, and all of the data were reported as radiance (photons/s/sr/cm^2). The intensity of each group was recorded to determine the percentage of tumor growth inhibition and antitumor efficacy. Tumor growth inhibition [(TGI, %)=(1–change of tumor volume in treatment group/change of tumor volume in control group)×100] was used to determine the percentage of tumor growth inhibition and antitumor efficacy.

PK/PD study

The mice were randomized into two groups, receiving a single dose of either vehicle control (n=3 per time point) or 30 mg/kg afatinib (n=per time point). At the time points 0.5, 1, 2, 8, and 24 h after dosing, the animals were humanely sacrificed, and the samples were harvested. Total blood was collected by intracardiac puncture, and the plasma layer was obtained by centrifugation at 1500×g for 15 min. CSF was collected by insertion of a 1-mL syringe into the dura through the atlanto-occipital membrane at a 30° angle. Plasma and CSF were stored at -80 °C until PK analysis. Afatinib was analyzed by high-performance liquid chromatography coupled with tandem mass spectrometry (HPLC-MS/MS)[9]. Solid-phase extraction was performed on plasma samples before the extract was injected into the HPLC-MS/MS instrument. CSF samples were injected directly without a prior extraction step. Chromatographic and mass spectrometric conditions were identical for both matrices. The samples were subjected to chromatography on a reversed-phase analytical HPLC column with gradient elution. Afatinib and the internal standard were detected by MS/MS using electrospray ionization in the positive mode. Calibration ranges were linear from 0.500 to 250 ng/mL for plasma and from 0.100 to 20.0 ng/mL for CSF. Brain tumors were collected at each time point and were fixed in 10% buffered formalin for 24 h and then embedded in paraffin for immunohistochemical (IHC) staining. To calculate the PK/PD parameters, standard non-compartmental methods and the E_{max} model were adopted; PKSolver software was used for these calculations.

Immunohistochemistry analysis

Antigen retrieval was conducted on formalin-fixed, paraffin-embedded tissue (FFPE) sections for 5 min with retrieval buffer (DAKO, Glostrup, Denmark), and the samples were then washed in running water for 5 min. Tissue samples were then rinsed in Tris buffered saline containing 1% Tween (TBST) and were incubated with an endogenous peroxidase blocker on a LabVision autostainer for 10 min. The slides were washed twice in TBST and incubated with primary antibodies (pEGFR, Abcam) for 60 min at room temperature and were then washed twice with TBST. The DAKO EnVision™+ System-HRP was used as the secondary antibody for vitalization, and staining was detected using diaminobenzidine (DAKO). Then, 15 min after streptavidin-peroxidase treatment and washing with TBST, the slides were counterstained with 4′,6-diamidino-2-phenylindoleand (DAPI) and visualized by chemiluminescence as described above[10]. To analyze the baseline expression or modulation, IHC scoring of pEGFR was conducted by using the following formula: scoring=0×[% cells with no staining (0)]+1×[% cells with faint to barely visible staining (1+)]+2×[% cells with weak to moderate staining (2+)]+3×[% cells with strong staining (3+)]. This method combined positive intensity with the percentage of tumor cell staining, and results were evaluated independently by two pathologists using microscopy.

Statistical analysis

Two-way analysis of variance (ANOVA) was adopted to compare the afatinib concentrations between mice with BMs and normal mice at different time points. Student's t tests were used to determine the significant differences between the survival of mice in the various experimental and control groups. Partial correlations that control for different time points were used to compare the correlation of afatinib concentration between the plasma and CSF. A P value less than 0.05 was considered to be significant.

Results

Establishment of the BM model

No obvious morphologic changes were observed between PC-9.luc cells and PC-9 cells. We also observed that PC-9.luc cells, compared with PC-9 cells, had a similar cell cycle distribution, growth kinetics, and cell doubling time (32.6±3.2 *vs* 31.9±3.3 h) (Supplementary Figure S1). This BM model was established in nude mice by the administration of PC-9.luc cells via intra-cerebral injection. No obvious changes in body weight were observed after surgery. Figure 1A shows the bioluminescence imaging (BLI) 14 d after the tumor cells were injected. The BLI signal reached 4.36×10^6 p/s/sr/cm^2 with an 18-fold increase compared with the baseline of 2.40×10^5 p/s/sr/cm^2 (Supplemental Figure S2). H&E staining was also performed on the brain tissue to evaluate the pathologic status (Figure 1B). A localized tumor focus was observed, and the margin between the focus and normal tissue was relatively clear. The peak concentrations of afatinib in the C_{CSF} of BM mice and normal mice were 17.48±1.50 nmol/L and 14.01±3.03 nmol/L, respectively, 1 h after the initial administration (Figure 1C). The concentration of afatinib in the C_{CSF} of BM and normal mice decreased at 2 h (3.40±0.90 nmol/L and 2.87±1.54 nmol/L), 8 h (0.27±0.09 nmol/L and 0.31±0.06 nmol/L) and 24 h (0.10±0.18 nmol/L and 0.04±0.07 nmol/L). The C_{CSF} values of the two groups demonstrated no significant difference (F=1.91, P=0.181) (Figure 1C). Although the stereotactic injection BM model has the potential to induce BBB damage, our results indicated that the BBB was still intact. Moreover, we did not observe any significant behavior disorders after an intracranial injection of 10 μL of liquid. Therefore, we determined that it was feasible to perform further research using this BM model.

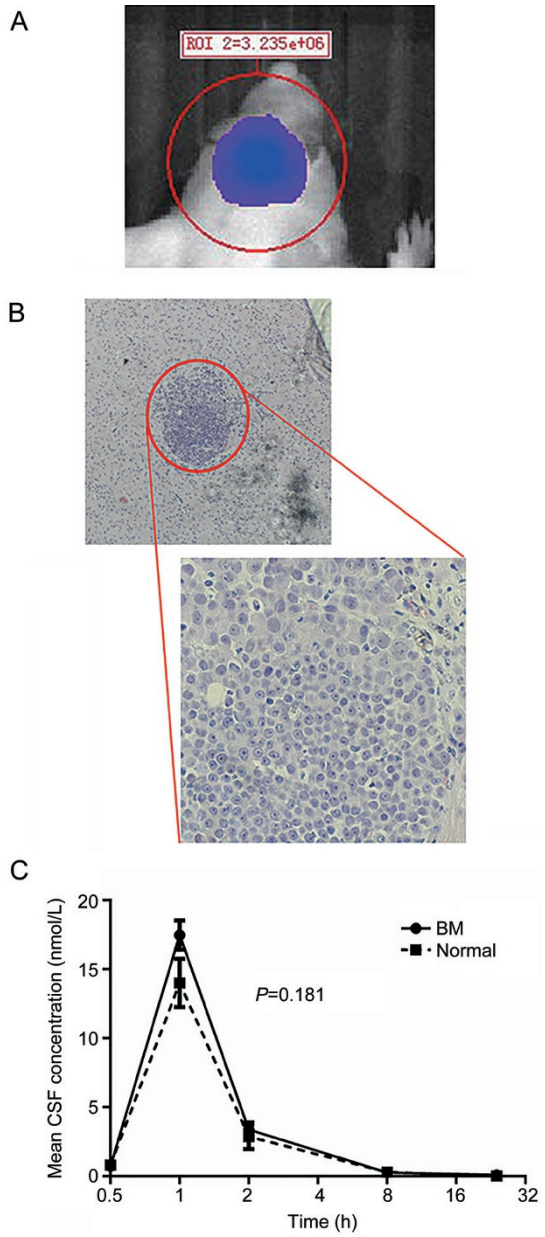

Figure 1. Validation of the established BM model. (A) A representative bioluminescence image 14 d after 1.0×10^6 PC-9 cells were injected. (B) H&E staining in brain tissues. (C) Comparison of the CSF concentration after the administration of 30 mg/kg afatinib to BM and normal mice (n=3/time point/group). Mean±SEM.

Afatinib inhibited the growth of intracranial tumors

After the feasibility of the BM model was verified, we evaluated the efficacy of afatinib in mice with BMs. The effects of two doses of afatinib (30 and 15 mg/kg) and one vehicle control were assessed to evaluate the dose-response relationship. During the development of BM, tumor growth was monitored using bioluminescence imaging (Figure 2A). The tumor burden in animals treated with vehicle increased by nearly 4-fold on d 7 (16.71×10^6 p/s/sr/cm^2) and continued to increase by nearly 20-fold on d 14 (85.22×10^6 p/s/sr/cm^2) compared with the tumor burden on d 0 (4.15×10^6 p/s/sr/cm^2) (Figure 2B). Regarding afatinib treatment, the administration of 15 mg/kg afatinib inhibited the *in vivo* growth of PC-9-derived tumors in the brain, because the TGI rates were 79.8% and 90.2% on d 7 (7.11×10^6 p/s/sr/cm^2) and d 14 (12.54×10^6 p/s/sr/cm^2), respectively. When the afatinib dose was increased to 30 mg/kg, tumor growth inhibition was further enhanced, and the TGI rate was 124.7% on d 7, thus indicating tumor regression on d 14 (Figure 2C). The BLI signal was 1.23×10^6 p/s/sr/cm^2 and 2.7×10^5 p/s/sr/cm^2 on d 7 and d 14, respectively (Figure 2A).

PK/PD parameters of afatinib in a PC-9 brain metastasis model

Our data showed that BM mice achieved tumor regression after treatment with 30 mg/kg afatinib. We then detected the concentrations of afatinib in the CSF and plasma at different time points to analyze the pharmacokinetic characteristics of this drug. The plasma concentration of afatinib was 91.4±31.2 nmol/L 0.5 h after injection and reached a peak (417.1±119.9 nmol/L) 1 h after injection. Then, the plasma concentration started to decrease over time. At 24 h, afatinib was detected at low levels. The concentration of afatinib in the CSF followed a similar pattern, with 0.74±0.43 nmol/L measured 0.5 h after injection; the concentration reached a peak (17.5±1.50 nmol/L) 1 h after injection (Figure 3A). The $t_{1/2}$ values in the plasma and CSF were 5.0 h and 3.7 h, respectively. The $AUC_{(0\text{–}24\ h)}$ values in the plasma and CSF were 2375.5 nmol/h and 29.1 nmol/h, respectively, whereas the ratio of AUC_{CSF}/AUC_{Plasma} was 1.23%. The Pearson correlation coefficient between the plasma and CSF concentrations of afatinib was 0.844, thus indicating a strong positive correlation (P<0.01, Figure 3A). The ratio of C_{CSF} to C_{plasma} was 0.8% (0.5 h after injection) and 4.2% (1 h after injection), and it then decreased over time (Figure 3B).

To study the pharmacodynamics of afatinib, we detected the expression of pEGFR (Tyr1068) in brain tumor foci by immunohistochemistry. Figure 4A shows the IHC result of pEGFR. One hour after the administration of 30 mg/kg afatinib, the pEGFR signal was reduced by 90%. The sustained inhibition of pEGFR was observed at 8 h and gradually recovered after 24 h. A positive correlation between the concentration of afatinib in the CSF and pEGFR modulation was observed (Figure 4B). The E_{max} model was used to determine the relationship between the concentration of afatinib in the CSF and pEGFR (Figure 5). The E_{max} was 86.5%, and the EC_{50} was 0.26 nmol/L.

Discussion

Currently, few effective treatment options exist for BM[11, 12]. The slow progress in the development of BM therapy might be due to the lack of suitable research models. In this study, we established a BM model in mice, which affords an opportunity to investigate BM. Various methods have been developed to establish BM models, among which the internal carotid artery injection (ICA) and the stereotactic injection techniques are the two most common approaches[13]. Our study adopted the stereotactic injection method to investigate the efficacy of afatinib

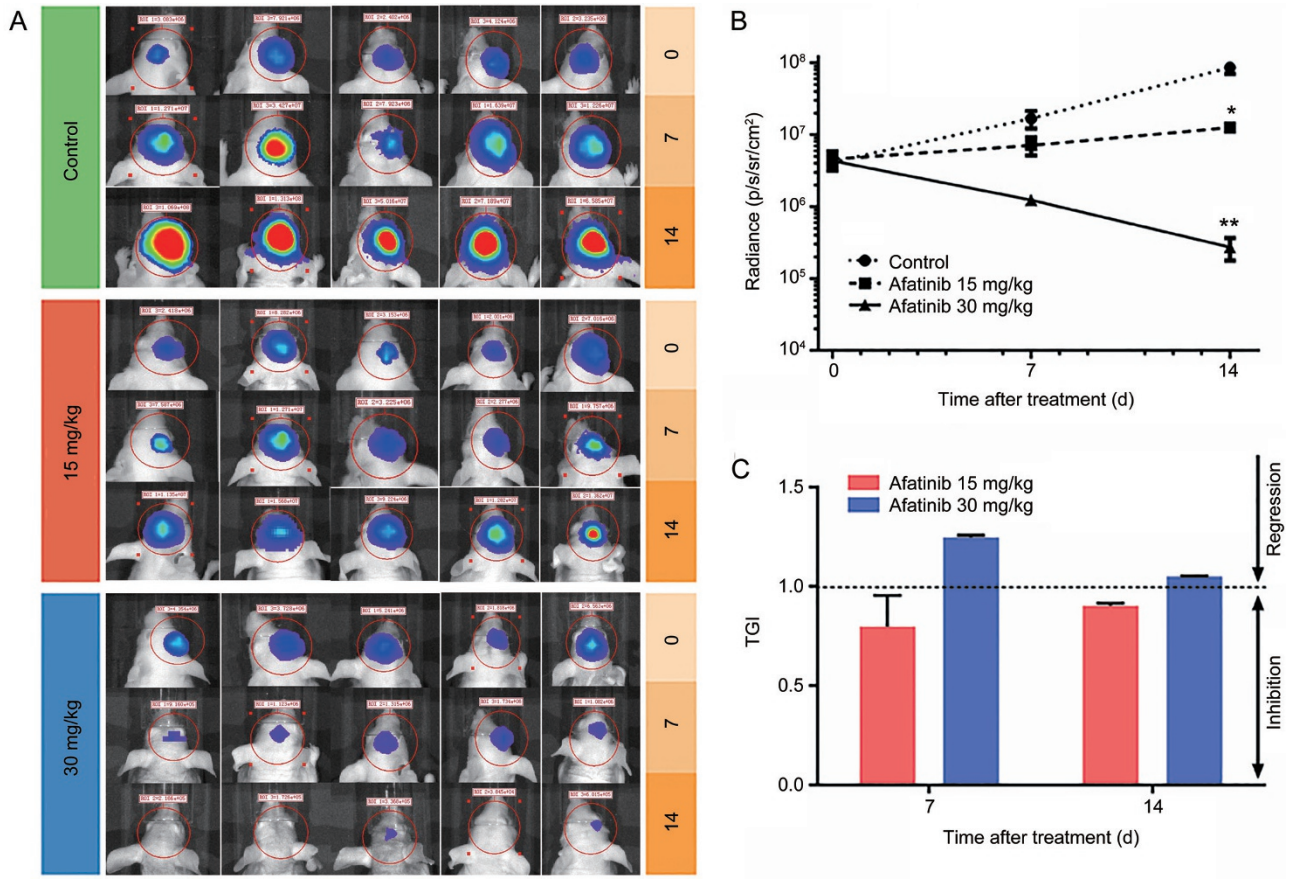

Figure 2. Effects of different doses of afatinib on BMs in mice. (A) Bioluminescence imaging of mice bearing brain metastases on d 0, 7, 14 after treatment with the different doses of afatinib and the vehicle control. (B) Mean radiance versus time by treatment in mice exhibiting brain metastases. Treatment was initiated on d 0 (n=5/time point/group). (C) Tumor growth inhibitory rate of low and high dose administration of afatinib at different time points. Mean±SEM.

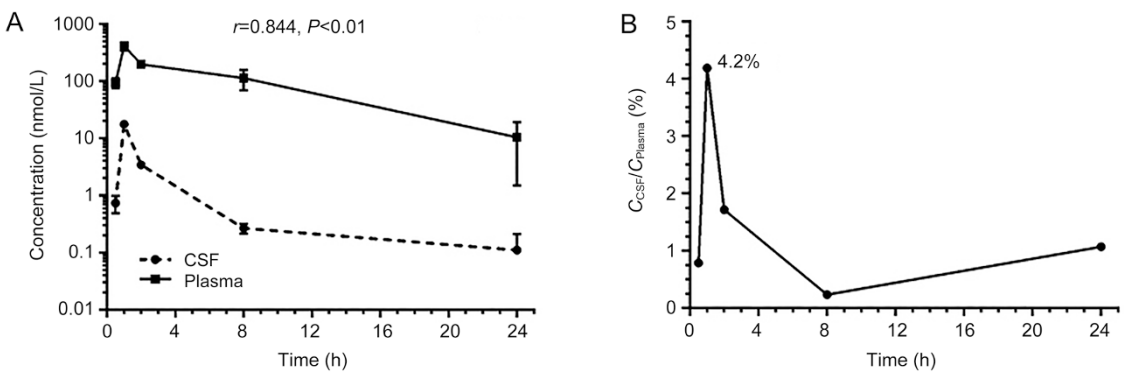

Figure 3. Pharmacokinetic analysis of afatinib in the PC-9 brain metastasis model. (A) Concentrations of afatinib against time in blood and cerebral spinal fluid (CSF); samples were collected 0.5, 2, 8, and 24 h after the administration of 30 mg/kg afatinib (n=3/time point). (B) Ratio of afatinib exposure in CSF and plasma 0.5, 2, 8, and 24 h after the administration of 30 mg/kg afatinib. Mean±SEM.

in BMs of lung cancer. BMs were successfully established in 30 of 30 mice, thus suggesting that our model is reliable. According to the pathological assessment, tumor nodules were identified in 100% of the mice. The internal carotid artery injection method reflects the hematogenous metastasis that mimics the natural process of BM. This method is the most technically challenging, because it requires extensive practice to master the microsurgical dissection and slow injection of

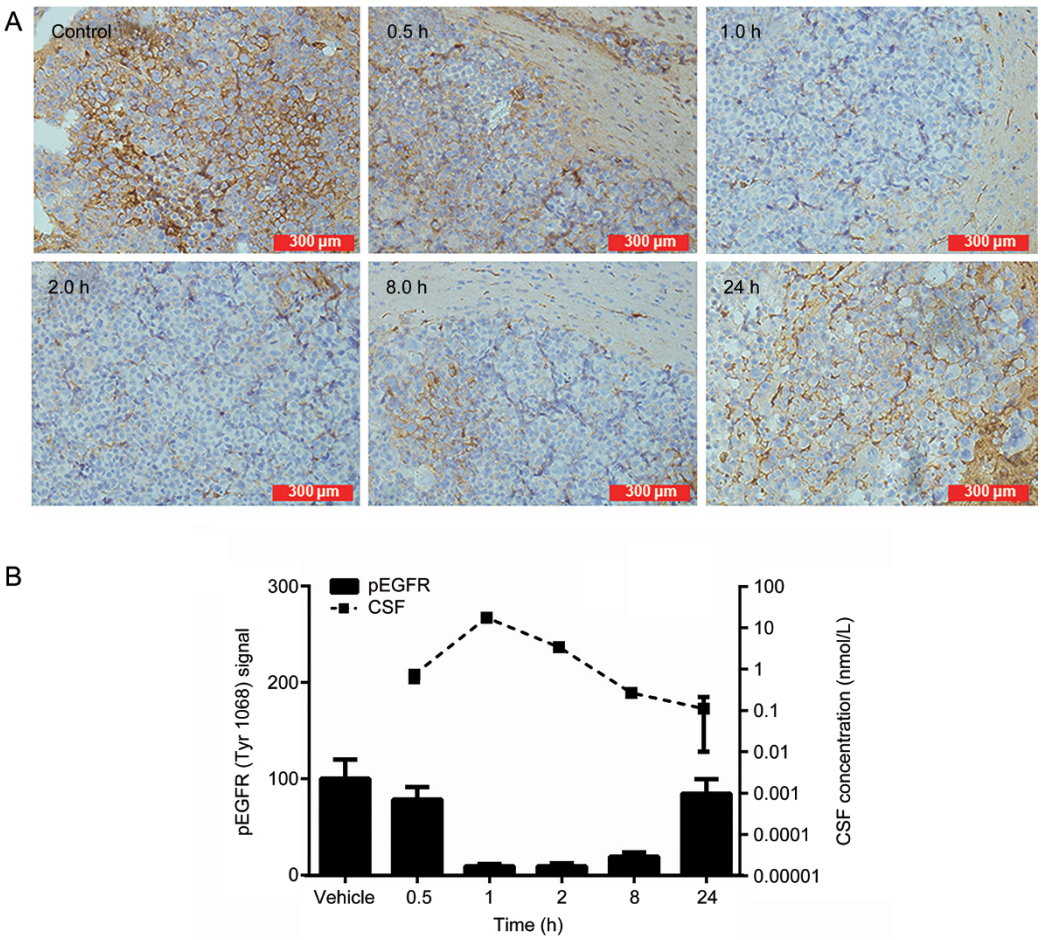

Figure 4. Pharmacokinetic and pharmacodynamics correlation of afatinib in the PC-9 brain metastasis model. (A) IHC revealed modulation of pEGFR in tumor tissue 0.5, 1, 2, 8, and 24 h after administration of 30 mg/kg afatinib. (B) A trend showing a positive correlation between CSF concentration and pEGFR modulation was identified (n=3/time point). Mean±SEM.

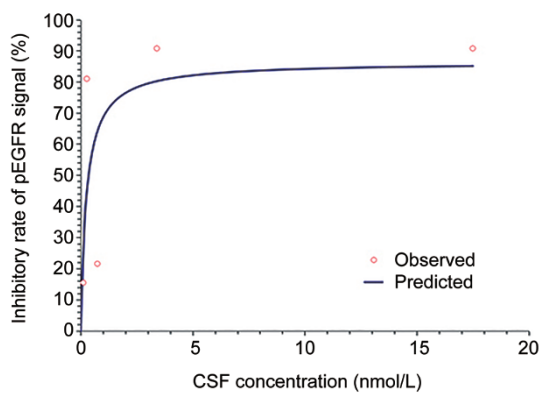

Figure 5. E_{max} model of the relationship between CSF concentration and pEGFR.

a cell suspension[14]. Do *et al* have repeated this method in 29 mice; four revealed no bioluminescence as a lower concentration of 2.5×10^5 cells injected, three died intraoperatively, owing to hemorrhage, three died within 7 d of the procedure, and only 19 mice developed tumors over 42 d post-injection[15]. In addition, the ICA-derived BM model has been reproduced with only a few human cell lines. In contrast, stereotactic injection models are easier to execute and are better tolerated by the animals. Of course, the stereotactic injection model carries the potential risk of damage to the integrity of the BBB. Through the detection of afatinib in the C_{CSF} after an injection of the same dose, we found no significant difference (F=2.44, P=0.216) between normal mice and BM mice, thus suggesting that the stereotactic injection did not damage the integrity of

Table 1. IC_{50} values of reversible EGFR-TKIs and afatinib.

	EGFR L858R		EGFR Exon 19 deletion	
	H3255	H1975 EGFR T790M	PC-9	PC-9/VanR EGFR T790M
Afatinib (nmol/L)	0.9	22	0.6	3
Gefitinib (nmol/L)	11.5	3102	7	741
Erlotinib (nmol/L)	9.5	6073	6	1262

Excerpt from Hoffknecht *et al*[6].

the BBB.

We then investigated the efficacy of afatinib in BMs from NSCLC. The administration of afatinib contributed to significant tumor inhibition and even tumor regression at higher doses. The levels of pEGFR modulations were correlated with the concentration of afatinib in the CSF (P<0.01), thus indicating that afatinib's tumor inhibitory effect is the result of targeting EGFR pathway. Our data demonstrated that the administration of 30 mg/kg afatinib nearly eliminated tumor cells by d 14. As a second-generation EGFR-TKI, afatinib is an irreversible EGFR-TKI and exhibits a strong affinity for ErbB receptors. Table 1 summarizes the inhibitory concentrations of currently available EGFR-TKIs for different mutation types *in vitro*[6, 16]. The lower IC_{50} value indicates that afatinib is more potent than first-generation TKIs. Afatinib primarily binds to albumin in the plasma, and its binding ratio is more than 92% in mice and approximately 95% in humans[17–19]. Low albumin concentrations in the CSF contribute to unbound afatinib as the primary form. As such, the PD analysis showed the EC_{50} of afatinib was 0.26 nmol/L, a value similar to the *in vitro* IC_{50} (0.28 nmol/L) of PC-9 cells reported in our previous work[20].

EGFR-TKIs are a class of small molecules that permeate across the BBB by two mechanisms: the lipophilic passive pathway and the receptor-mediated active transport pathway[21]. The disrupted BBB in the presence of BM leads to an increased passive transport of TKIs. The peak penetration rate of afatinib was 4.2% in this study (Figure 3B). In contrast, the rates are 0.6%–1.3% for gefitinib and 2.8%–4.4% for erlotinib[10, 22–24]. A pooled analysis of the results from the LUX-Lung3 and LUX-Lung6 studies by Schuler *et al* has shown that, compared with chemotherapy, first-line afatinib improves the PFS in EGFR mutation-positive NSCLC patients with BM[5]. Although the penetration rate of afatinib was similar to that of erlotinib, the IC_{50} of afatinib was only 10% that of erlotinib. The LUX-Lung8 study revealed significant improvements in progression-free survival and overall survival with afatinib treatment compared with erlotinib treatment in patients with squamous cell carcinoma of the lung[25]. Additionally, afatinib exhibited encouraging efficacy in patients after the failure of first-generation EGFR-TKIs. Schuler *et al* have retrospectively analyzed the efficacy of afatinib in 571 patients after the failure of EGFR-TKIs. The authors have found that afatinib results in a median time to treatment failure (TTF) of 4.0 months in patients with adenocarcinomas compared with extensively pretreated NSCLC patients. Additionally, for patients with EGFR-mutated NSCLC, a longer TTF of 4.6 months has been achieved[26]. We elected to use a dose of 15–30 mg/kg once daily for 14 d in mice. Given the dose coefficient between humans and mice, the dose intensity of 15 mg/kg of afatinib in our study is equivalent to 46.2 mg daily in humans, which is tolerable.

Afatinib has a moderate capacity to permeate the BBB, whereas the majority of the drug is counteracted by P-glycoprotein, which is one of the efflux pumps located on the membrane of endothelial cells[21]. Therefore, the efficacy of single use afatinib for treatment of BMs is limited in the clinic. WBRT is the standard of care for BM, but efforts in the exploration of the combination of targeted therapy and WBRT are ongoing. Previous studies have shown the benefit and feasibility of combination EGFR-TKIs with WBRT[27, 28]. WBRT disrupts the BBB and leads to an increased passage of afatinib across the BBB via the passive pathway. Our previous work has shown that afatinib exhibits radiosensitization effects in PC-9 cells and PC-9 gefitinib-resistant cells with sensitization enhancement ratios (SERs) of 1.22 and 1.50, respectively[20]. Afatinib markedly blocked the basal level of EGFR and ERK phosphorylation and caused delays in the radiation-induced phosphorylation of AKT in lung cancer cells. In addition, afatinib enhanced radiation-induced apoptosis and caused a delay in DNA damage repair in PC-9 gefitinib-resistant cells through reduced DNA-pKcs expression. These data further support the possibility of treatments including a combination of WBRT and afatinib for patients with BMs of NSCLC.

In summary, the present study demonstrated the efficacy of afatinib in a BM mouse model using PC-9 cells. The observed efficacy correlated with the dose that was administered, because a high dose of afatinib led to BM regression. The concentration of afatinib in the plasma was correlated with that in the CSF, thus suggesting the feasibility of the administration of a high dose of afatinib. Furthermore, the afatinib concentration in the CSF was correlated with the modulation of pEGFR in tumor tissues. These findings provide evidence for the potential application of afatinib in NSCLC patients with BMs.

Acknowledgements

This work was supported by funding from the National Natural Science Foundation of China (81272611), the Zhejiang Provincial Foundation of Natural Science (LZ13H60001) and the Major Science and Technology Innovation Project of Hangzhou (20112312A01) to Sheng-lin MA and the Zhejiang Medical Science Foundation, China (2014KYA178), the Hangzhou Key Disease and Discipline Foundation, China (20140733Q15), and the Zhejiang Provincial Natural Science Foundation of China (LY15H160010) to Shi-rong ZHANG.

Author contribution

Sheng-lin MA, Bing XIA, and Shi-rong ZHANG designed the research; Lu-cheng ZHU, Shi-rong ZHANG, Yan-ping JIANG, Jing ZHANG, Ru-jun XU, and Ya-si XU conducted the experiments; Lu-cheng ZHU and Shi-rong ZHANG performed the data analysis; Lu-cheng ZHU and Shi-rong ZHANG wrote the manuscript.

Supplementary information

Supplementary information is available at the website of Acta Pharmacologica Sinica.

References

1 Gavrilovic IT, Posner JB. Brain metastases: epidemiology and pathophysiology. J Neurooncol 2005; 75: 5–14.

2 Mujoomdar A, Austin JH, Malhotra R, Powell CA, Pearson GD, Shiau MC, *et al*. Clinical predictors of metastatic disease to the brain from

non-small cell lung carcinoma: primary tumor size, cell type, and lymph node metastases. Radiology 2007; 242: 882–8.
3 Kawabe T, Phi JH, Yamamoto M, Kim DG, Barfod BE, Urakawa Y. Treatment of brain metastasis from lung cancer. Prog Neurol Surg 2012; 25: 148–55.
4 Li D, Ambrogio L, Shimamura T, Kubo S, Takahashi M, Chirieac LR, *et al.* BIBW2992, an irreversible EGFR/HER2 inhibitor highly effective in preclinical lung cancer models. Oncogene 2008; 27: 4702–11.
5 Schuler M, Wu YL, Hirsh V, O'Byrne K, Yamamoto N, Mok T, *et al.* First-line afatinib versus chemotherapy in patients with non-small cell lung cancer and common epidermal growth factor receptor gene mutations and brain metastases. J Thorac Oncol 2016; 11: 380–90.
6 Hoffknecht P, Tufman A, Wehler T, Pelzer T, Wiewrodt R, Schutz M, *et al.* Efficacy of the irreversible ErbB family blocker afatinib in epidermal growth factor receptor (EGFR) tyrosine kinase inhibitor (TKI)-pretreated non-small-cell lung cancer patients with brain metastases or leptomeningeal disease. J Thorac Oncol 2015; 10: 156–63.
7 Clark AJ, Safaee M, Oh T, Ivan ME, Parimi V, Hashizume R, *et al.* Stable luciferase expression does not alter immunologic or *in vivo* growth properties of GL261 murine glioma cells. J Transl Med 2014; 12: 345.
8 Zeng Q, Wang J, Cheng Z, Chen K, Johnstrom P, Varnas K, *et al.* Discovery and evaluation of clinical candidate AZD3759, a potent, oral active, central nervous system-penetrant, epidermal growth factor receptor tyrosine kinase inhibitor. J Med Chem 2015; 58: 8200–15.
9 Fouad M, Helvenstein M, Blankert B. Ultra high performance liquid chromatography method for the determination of two recently FDA approved TKIs in human plasma using diode array detection. J Anal Methods Chem 2015; 2015: 215128.
10 Chen Y, Wang M, Zhong W, Zhao J. Pharmacokinetic and pharmacodynamic study of Gefitinib in a mouse model of non-small-cell lung carcinoma with brain metastasis. Lung Cancer 2013; 82: 313–8.
11 Haughton ME, Chan MD, Watabe K, Bonomi M, Debinski W, Lesser GJ, *et al.* Treatment of brain metastases of lung cancer in the era of precision medicine. Front Biosci (Elite Ed) 2016; 8: 219–32.
12 Nussbaum ES, Djalilian HR, Cho KH, Hall WA. Brain metastases. Histology, multiplicity, surgery, and survival. Cancer 1996; 78: 1781–8.
13 Saito N, Hatori T, Murata N, Zhang ZA, Nonaka H, Aoki K, *et al.* Comparison of metastatic brain tumour models using three different methods: the morphological role of the pia mater. Int J Exp Pathol 2008; 89: 38–44.
14 Chua JY, Pendharkar AV, Wang N, Choi R, Andres RH, Gaeta X, *et al.* Intra-arterial injection of neural stem cells using a microneedle technique does not cause microembolic strokes. J Cereb Blood Flow Metab 2011; 31: 1263–71.
15 Do J, Foster D, Renier C, Vogel H, Rosenblum S, Doyle TC, *et al. Ex vivo* Evans blue assessment of the blood brain barrier in three breast cancer brain metastasis models. Breast Cancer Res Treat 2014; 144: 93–101.
16 Cross DA, Ashton SE, Ghiorghiu S, Eberlein C, Nebhan CA, Spitzler PJ, *et al.* AZD9291, an irreversible EGFR TKI, overcomes T790M-mediated resistance to EGFR inhibitors in lung cancer. Cancer Discov 2014; 4: 1046–61.
17 Wiebe S, Schnell D, Kulzer R, Gansser D, Weber A, Wallenstein G, *et al.* Influence of renal impairment on the pharmacokinetics of afatinib: an open-label, single-dose study. Eur J Drug Metab Pharmacokinet 2016. doi: 10.1007/s13318-016-0359-9.
18 Schnell D, Buschke S, Fuchs H, Gansser D, Goeldner RG, Uttenreuther-Fischer M, *et al.* Pharmacokinetics of afatinib in subjects with mild or moderate hepatic impairment. Cancer Chemother Pharmacol 2014; 74: 267–75.
19 Wind S, Schnell D, Ebner T, Freiwald M, Stopfer P. Clinical pharmacokinetics and pharmacodynamics of afatinib. Clin Pharmacokinet 2016. doi: 10.1007/s40262-016-0440-1.
20 Zhang S, Zheng X, Huang H, Wu K, Wang B, Chen X, *et al.* Afatinib increases sensitivity to radiation in non-small cell lung cancer cells with acquired EGFR T790M mutation. Oncotarget 2015; 6: 5832–45.
21 Zhang J, Yu J, Sun X, Meng X. Epidermal growth factor receptor tyrosine kinase inhibitors in the treatment of central nerve system metastases from non-small cell lung cancer. Cancer Lett 2014; 351: 6–12.
22 Zhao J, Chen M, Zhong W, Zhang L, Li L, Xiao Y, *et al.* Cerebrospinal fluid concentrations of gefitinib in patients with lung adenocarcinoma. Clin Lung Cancer 2013; 14: 188–93.
23 Togashi Y, Masago K, Masuda S, Mizuno T, Fukudo M, Ikemi Y, *et al.* Cerebrospinal fluid concentration of gefitinib and erlotinib in patients with non-small cell lung cancer. Cancer Chemother Pharmacol 2012; 70: 399–405.
24 Deng Y, Feng W, Wu J, Chen Z, Tang Y, Zhang H, *et al.* The concentration of erlotinib in the cerebrospinal fluid of patients with brain metastasis from non-small-cell lung cancer. Mol Clin Oncol 2014; 2: 116–20.
25 Soria JC, Felip E, Cobo M, Lu S, Syrigos K, Lee KH, *et al.* Afatinib versus erlotinib as second-line treatment of patients with advanced squamous cell carcinoma of the lung (LUX-Lung 8): an open-label randomised controlled phase 3 trial. Lancet Oncol 2015; 16: 897–907.
26 Schuler M, Fischer JR, Grohe C, Gutz S, Thomas M, Kimmich M, *et al.* Experience with afatinib in patients with non-small cell lung cancer progressing after clinical benefit from gefitinib and erlotinib. Oncologist 2014; 19: 1100–9.
27 Zeng YD, Zhang L, Liao H, Liang Y, Xu F, Liu JL, *et al.* Gefitinib alone or with concomitant whole brain radiotherapy for patients with brain metastasis from non-small-cell lung cancer: a retrospective study. Asian Pac J Cancer Prev 2012; 13: 909–14.
28 Welsh JW, Komaki R, Amini A, Munsell MF, Unger W, Allen PK, *et al.* Phase II trial of erlotinib plus concurrent whole-brain radiation therapy for patients with brain metastases from non-small-cell lung cancer. J Clin Oncol 2013; 31: 895–902.